CrossMark

ORIGINAL ARTICLE

Analytic propagation of near-circular satellite orbits in the atmosphere of an oblate planet

**Vladimir Martinusi[1] · Lamberto Dell'Elce[1] ·
Gaëtan Kerschen[1]**

Abstract In the present paper, an averaging perturbation technique leads to the determination of a time-explicit analytic approximate solution for the motion of a low-Earth-orbiting satellite . The two dominant perturbations are taken into account: the Earth oblateness and the atmospheric drag. The proposed orbit propagation algorithm comprises the Brouwer–Lyddane transformation (direct and inverse), coupled with the analytic solution of the averaged equations of motion. This solution, based on equinoctial elements, is singularity-free, and therefore it stands for low inclinations and small eccentricities as well. The simplifying assumption of a constant atmospheric density is made, which is reasonable for near-circular orbits and short-time orbit propagation. Two sets of time-explicit equations are provided, for moderate and small eccentricities ($\mathcal{O}(e^4) = 0$ and $\mathcal{O}(e^2) = 0$, respectively), and they are obtained by performing (1) a regularization of the original averaged differential equations of motion for the vectorial orbital elements, and (2) Taylor series expansions of the aforementioned equations with respect to the eccentricity. The numerical simulations show that the errors due to the use of the proposed analytic model in the presence of drag are almost the same as the errors of the Brouwer first-order approximation in the absence of drag.

✉ Vladimir Martinusi
  vladimir.martinusi@ulg.ac.be

  Lamberto Dell'Elce
  lamberto.dellelce@ulg.ac.be

  Gaëtan Kerschen
  g.kerschen@ulg.ac.be

[1] Space Structures and Systems Lab, Department of Aerospace and Mechanical Engineering,
  University of Liège, Liège, Belgium

1 Introduction

The main perturbations acting upon low-Earth orbiting satellites are due to the planet's oblateness and the presence of the atmosphere. Their combined effect causes the orbit to dramatically drift from the Keplerian unperturbed model. While the oblateness perturbation (where the dominant term depends on the J_2 zonal harmonic) still falls in the range of conservative forces, allowing the classic perturbation methods to be applied, the atmospheric drag produces a non-conservative force, making the use of the tools of analytic mechanics difficult.

While the search for analytic models that approximate the motion of a satellite about an oblate planet (approach known as "the main problem in artificial satellite theory") brought a multitude of solutions: Garfinkel (1959), Brouwer (1959), Kozai (1959), Lyddane (1963), Vinti (1960), Cid and Lahulla (1969), Deprit (1981), Gurfil and Lara (2014), Lara et al. (2014), the analytic solutions for the atmospheric drag are present in a much less significant amount.

The study of the effect of atmospheric drag on satellites' orbits dates back to the first years of the spaceflight era. One of the initial and most important contributions in this area belongs to King-Hele (1964). Although the effects of the atmospheric drag were approached thoroughly, the effects of the other perturbations were neglected. Battin (1999) developed closed-form expressions for the averaged variation of semimajor axis and eccentricity in terms of modified Bessel functions of the first kind. Vallado and McClain (2001) and Roy (2004) presented approximate variational equations for eccentricity and semimajor axis, deriving expressions for the secular rates of change of the orbital elements which are suitable for series expansion in powers of the eccentricity. Mittleman and Jezewski (1982) offered the solution to a modified problem, where an approximate expression for the drag acceleration was used such that the problem becomes integrable. Vinh et al. (1979) also derived closed-form expressions for the variational equations of the orbital elements with respect to a new independent variable, and then used numerical techniques to integrate the equations of motion. All the aforementioned studies either treat the atmospheric drag exclusively, and hence ignore the other dominant perturbation, namely the Earth's oblateness, or do not provide an analytic solution, but offer instead numerical techniques to integrate them.

Combining the effects of the two major perturbations seems quite a challenge, and few attempts were made so far. Brouwer and Hori (1961) extended the Poincaré-von Zeipel-based method developed previously by Brouwer (1959) to accommodate the atmospheric drag, failing to reach closed-form equations of motion, but rather focusing on the separation of the variables in order to ease numerical integration. Parks (1983) included the averaged effects of the atmospheric drag in the contact transformation developed in Brouwer (1959), but this method of solution rises several issues regarding the invertibility of the contact transformation, which is essentially needed for propagating the osculating elements. Franco (1991) developed an approximate model for the motion about an oblate planet with atmosphere, but only for the equatorial case.

In this context, the objective of this paper is to derive a new time-explicit solution of the problem combining the J_2 and drag forces. The outcome is an analytic short-term propagator which could be implemented onboard the satellite.[1] To support this conjecture, numerical simulations show that the error in position, after two days of propagation of a low Earth orbit with an initial altitude of 350 km and a ballistic coefficient $C_B = 0.022$ m^2 kg, with a

---

[1] Due to the presence of significant uncertainties in the atmosphere (influence of the solar activity, day/night density variations, the atmospheric bulge, winds), realistic long-term propagations in the presence of drag cannot be addressed with deterministic tools [see Dell'Elce and Kerschen (2014)].

(constant) density $\rho_0 = 10^{-11}$ kg/m^3, reaches hundreds of kilometers if the effects of the atmospheric drag are ignored.

The present approach is based on the so-called perturbation averaging method, which is in fact an expansion in trigonometric series (with respect to the mean anomaly) where only the first term is retained. This approach already exists for the J_2-only perturbation, namely the Brouwer first-order model, and it is possible to develop it by simple manipulations, as in Hestenes (1999) and Condurache et al. (2013). The same averaging technique can be applied to the drag acceleration, obtaining the variational equations for the orbital elements with the combined effect of J_2 and drag. By making the assumptions that (1) the atmospheric density is constant and (2) the orbit eccentricity is small (both situations $\mathcal{O}(e^2) \simeq 0$ and $\mathcal{O}(e^4) \simeq 0$ are addressed), *time-explicit solutions to the equations of motion for the averaged classic orbital elements* are obtained.

The essential remark regarding this approach is that, after averaging, the new variational equations do not refer to the osculating orbital elements (and their choice may be made among several types; if the system is Hamiltonian, a set of canonical elements will obviously be used), but for a new set of elements, which corresponds to the new dynamical problem. They are usually referred to as *mean elements* in Astrodynamics [see Cain (1962)], or *new variables* in classical mechanics. When treating a perturbation in this way, a connection between the *old* and the *new variables* needs to be established, and it is made via a *canonical contact transformation* (the term "contact" indicating a change of coordinates in the phase space involving both the generalized coordinates and the conjugate momenta). It may be either of the Jacobian type [(as in the Poincaré-von Zeipel method, used by Brouwer (1959)], or infinitesimal, as in the method used by Deprit (1969, 1981).

The main challenge in the J_2 & drag problem is that the system is non-conservative. However, the assumption that for short-term orbit prediction the canonical contact transformation corresponding to the Hamiltonian system (in this case the J_2-only dynamical system) can be used to travel between the old and the new variables appears legitimate. In other words, the new dynamical system, corresponding to the averaged equations of motion, takes into account the effects of the atmospheric drag, and only the transformation back to the (approximate) osculating elements is made by ignoring the drag effect.

The paper is organized as follows. Section 2 introduces the model for the motion of a satellite under the influence of J_2 and drag, under the assumption of a static uniform atmosphere, and defines the quantities related to the associated unperturbed Keplerian problem for which variational equations will be developed. The averaged differential equations for the variational elements, together with some qualitative and quantitative insights of the motion, are offered. Section 3 presents the time-explicit solution for the equations of motion, for small ($e^4 \simeq 0$) and very small ($e^2 \simeq 0$) eccentricities. To the knowledge of the Authors, no time-explicit solution for the problem in discussion was developed to date. Section 4 describes the algorithm for orbit propagation. Section 5 presents the validation of the developed model, by exploring a broad set of initial and atmospheric conditions, by means of a Monte-Carlo analysis. Section 6 presents the conclusions and the future directions of investigation.

2 Method of solution

2.1 Problem statement

The initial value problem governing the motion of a satellite about an oblate planet, under the influence of atmospheric drag, is:

$$\ddot{\mathbf{r}} + \frac{\mu}{r^3}\mathbf{r} = \mathbf{f}_d, \quad \mathbf{r}(t_0) = \mathbf{r}_0, \quad \dot{\mathbf{r}}(t_0) = \mathbf{v}_0, \quad \mathbf{f}_d = \mathbf{f}_{J_2} + \mathbf{f}_{drag} \tag{1}$$

where $\mathbf{f}_{J_2}$ and $\mathbf{f}_{drag}$ model the accelerations due to the oblateness and to the drag, respectively. The over-dot indicates the derivative with respect to the time variable $t \geq t_0$, where t_0 denotes the initial moment of time. The closed-form expressions of the perturbing accelerations are:

$$\mathbf{f}_{J_2} = -\frac{3k_2}{r^4}\left[\left(1 - 5\frac{z^2}{r^2}\right)\hat{\mathbf{r}} + 2\frac{z}{r}\mathbf{i}_z\right] \tag{2a}$$

$$\mathbf{f}_{drag} = -C_0 \|\dot{\mathbf{r}}\| \dot{\mathbf{r}} \tag{2b}$$

and the following notations are used:

$$k_2 = \frac{\mu J_2 r_{eq}^2}{2}, \quad C_0 = \frac{1}{2}C_D \frac{S_{ref}}{m}\rho_0$$

Here μ is the gravitational parameter, J_2 is the second zonal harmonic, $\mathbf{i}_z$ is the unit vector associated with the Earth's rotation axis, z is the projection of the position vector on the Earth's rotation axis, $z = \mathbf{r} \cdot \mathbf{i}_z$, while $\hat{\mathbf{r}}$ denotes the unit vector associated with vector $\mathbf{r}$; r_{eq} denotes the mean equatorial radius, C_D is the drag coefficient, S_{ref} is the cross-sectional area of the satellite, m is its mass and ρ_0 is the atmospheric density. The assumptions of a static uniform atmosphere (the effect of the Earth rotation is neglected), a constant drag coefficient and the presence of drag exclusively (no lift) are made [cf. Chao (2005)].

The unperturbed problem associated to the initial value problem (1) (for $\mathbf{f}_d = \mathbf{0}$) is Kepler's problem, which has the classic first integrals:

$$\mathbf{h} = \mathbf{r} \times \dot{\mathbf{r}}, \quad \mathbf{e} = \frac{1}{\mu}\dot{\mathbf{r}} \times \mathbf{h} - \hat{\mathbf{r}}, \quad \mathcal{E} = \frac{1}{2}\dot{\mathbf{r}}^2 - \frac{\mu}{r} \tag{3}$$

namely the specific angular momentum, the eccentricity vector and the specific total energy, respectively. If $\mathcal{E} < 0$, then the unperturbed trajectory is an ellipse with eccentricity e and semimajor axis $a = -\mu/(2\mathcal{E})$. The use of the vectorial orbital elements $\mathbf{h}$ and $\mathbf{e}$ together with the specific total energy $\mathcal{E}$ is inspired by Hestenes (1999) and Condurache et al. (2013), and is motivated by the intuitive geometric interpretations available even before solving the equations of motion.

2.2 Variational method and averaging

If the perturbing acceleration $\mathbf{f}_d$ is taken into account, the quantities defined in Eq. (3) are no longer constant. The motion may still be referred to these quantities, but their variations should be taken into account. A classic perturbation method of averaging is used, where the averages over one period of the unperturbed motion are computed for the former constants of the motion $\mathbf{h}$, $\mathbf{e}$ and $\mathcal{E}$. For computational purposes, it is more convenient to use the semimajor axis a instead of the specific energy $\mathcal{E}$. The derivatives of $\mathbf{h}$, $\mathbf{e}$ and a may be expressed as:

$$\dot{\mathbf{h}} = \mathbf{r} \times \mathbf{f}_d, \quad \dot{\mathbf{e}} = \frac{1}{\mu}\left[\mathbf{f}_d \times \mathbf{h} - (\mathbf{r} \times \mathbf{f}_d) \times \dot{\mathbf{r}}\right], \quad \dot{a} = \frac{2a^2}{\mu}(\dot{\mathbf{r}} \cdot \mathbf{f}_d) \tag{4}$$

Denote by T the main period of the unperturbed motion, and by n the mean motion. Then it holds:

$$T = \frac{2\pi}{\sqrt{\mu}}a^{3/2} = \frac{2\pi}{n}$$

The averages over one period T of the unperturbed motion of the derivatives expressed in Eq. (4) are defined as follows:

$$\dot{\overline{\mathbf{h}}} = \frac{1}{T} \int_0^T (\mathbf{r} \times \mathbf{f}_d)\, \mathrm{d}t \tag{5a}$$

$$\dot{\overline{\mathbf{e}}} = \frac{1}{\mu T} \int_0^T [\mathbf{f}_d \times \mathbf{h} - (\mathbf{r} \times \mathbf{f}_d) \times \dot{\mathbf{r}}]\, \mathrm{d}t \tag{5b}$$

$$\dot{\overline{a}} = \frac{2a^2}{\mu T} \int_0^T (\dot{\mathbf{r}} \cdot \mathbf{f}_d)\, \mathrm{d}t \tag{5c}$$

It is convenient to refer all the vector functions used in Eq. (5) to a reference frame, which classicly is chosen to be the averaged perifocal frame, defined by the orthogonal unit vectors $\{\overline{\mathbf{u}}_k\}_{k=1,2,3}$:

$$\overline{\mathbf{u}}_1 = \frac{\overline{\mathbf{e}}}{\|\overline{\mathbf{e}}\|}, \quad \overline{\mathbf{u}}_2 = \frac{\overline{\mathbf{h}} \times \overline{\mathbf{e}}}{\|\overline{\mathbf{h}}\| \|\overline{\mathbf{e}}\|}, \quad \overline{\mathbf{u}}_3 = \frac{\overline{\mathbf{h}}}{\|\overline{\mathbf{h}}\|}$$

All the vectors which are expressed as column matrices are referred to this particular reference frame, if no other specification is made. The position and velocity vectors in the perifocal frame are:

$$\mathbf{r} = r \begin{bmatrix} \cos f \\ \sin f \\ 0 \end{bmatrix}; \quad \mathbf{v} = \frac{h}{p} \begin{bmatrix} -\sin f \\ e + \cos f \\ 0 \end{bmatrix}$$

if expressed with respect to the true anomaly, and:

$$\mathbf{r} = \begin{bmatrix} a\,(\cos E - e) \\ b \sin E \\ 0 \end{bmatrix}; \quad \mathbf{v} = \frac{na}{r} \begin{bmatrix} -a \sin E \\ b \cos E \\ 0 \end{bmatrix}$$

if expressed with respect to the eccentric anomaly.

In the right-hand side of Eq. (5), the expressions are linear with respect to $\mathbf{f}_d$, and therefore they may be separated as:

$$\frac{\mathrm{d}}{\mathrm{d}t}\overline{()} = \frac{\mathrm{d}}{\mathrm{d}t}\overline{()}_{J_2} + \frac{\mathrm{d}}{\mathrm{d}t}\overline{()}_{drag}$$

The expressions of $\dot{\overline{\mathbf{h}}}_{J_2}$, $\dot{\overline{\mathbf{e}}}_{J_2}$ and $\dot{\overline{a}}_{J_2}$ are computed as follows [see Condurache et al. (2013)]:

$$\dot{\overline{\mathbf{h}}}_{J_2} = -\frac{3k_2}{\overline{b}^3} (\mathbf{i}_z \cdot \overline{\mathbf{u}}_3)(\mathbf{i}_z \times \overline{\mathbf{u}}_3) \tag{6a}$$

$$\dot{\overline{\mathbf{e}}}_{J_2} = \frac{3\overline{e}k_2}{2\overline{h}\overline{b}^3} \left\{ -\left[1 - 3(\mathbf{i}_z \cdot \overline{\mathbf{u}}_3)^2\right]\overline{\mathbf{u}}_2 + 2(\mathbf{i}_z \cdot \overline{\mathbf{u}}_2)(\mathbf{i}_z \cdot \overline{\mathbf{u}}_3)\overline{\mathbf{u}}_3 \right\} \tag{6b}$$

$$\dot{\overline{a}}_{J_2} = 0 \tag{6c}$$

where

$$\overline{b} = \overline{a}\sqrt{1 - \overline{e}^2}$$

As expected, the magnitudes of vectors $\overline{\mathbf{h}}_{J_2}$ and $\overline{\mathbf{e}}_{J_2}$ remain constant, based on the fact that:

$$\frac{d}{dt} \left\| \overline{\mathbf{h}}_{J_2} \right\|^2 = 2\overline{h}_{J_2} \left(\overline{\mathbf{u}}_3 \cdot \dot{\overline{\mathbf{h}}}_{J_2} \right) = 0 \qquad \frac{d}{dt} \left\| \overline{\mathbf{e}}_{J_2} \right\|^2 = 2\overline{e}_{J_2} \left(\overline{\mathbf{u}}_1 \cdot \dot{\overline{\mathbf{e}}}_{J_2} \right) = 0$$

It follows that the magnitudes $\overline{h}$ and $\overline{e}$ are affected only by the atmospheric drag, and their derivatives are computed further in the current section.

Consider $K(\cdot)$ and $E(\cdot)$ the complete elliptic integrals of the first and second kinds, respectively, defined as [see Abramowitz and Stegun (1964)]:

$$K(w) = \int_0^1 \frac{du}{\sqrt{1 - w^2 u^2}}, \quad E(w) = \int_0^1 \frac{\sqrt{1 - u^2}}{\sqrt{1 - w^2 u^2}} du \quad 0 \le w \le 1$$

Then the variations of $\mathbf{h}$, $\mathbf{e}$ and a that are due to the atmospheric drag are computed from Eq. (5) by making use of the equality:

$$\frac{1}{T} \int_0^T \mathcal{F}(E(t)) \, dt = \frac{1}{2\pi a} \int_0^{2\pi} r \mathcal{F}(E) \, dE,$$

which is valid for any continuous vector or scalar function $\mathcal{F}$, and is deduced from $dE = (na/r)dt$. Denote:

$$\overline{p} = \overline{a} \left(1 - \overline{e}^2 \right), \quad \overline{n} = \sqrt{\mu} \overline{a}^{-3/2}$$

It follows:

$$\dot{\overline{\mathbf{h}}}_{drag} = \frac{-\mu C_0 \overline{b}}{2\pi \overline{a}} \left(\int_0^{2\pi} \sqrt{1 - e^2 \cos E} \, dE \right) \overline{\mathbf{u}}_3$$

$$\dot{\overline{\mathbf{e}}}_{drag} = -\frac{4\overline{n} \, \overline{p} C_0}{\pi} \left[\left(\int_0^{2\pi} \frac{\sqrt{1 - e^2 \cos E}}{1 - e \cos E} \cos E \, dE \right) \overline{\mathbf{u}}_1 \right.$$

$$\left. + \left(\frac{\overline{a}}{\overline{b}} \int_0^{2\pi} \frac{\sqrt{1 - e^2 \cos E}}{1 - e \cos E} \sin E \, dE \right) \overline{\mathbf{u}}_2 \right]$$

$$\dot{\overline{a}}_{drag} = -\frac{\overline{n} C_0}{2\pi} \int_0^{2\pi} \frac{\sqrt{1 - e^2 \cos E}}{1 - e \cos E} (1 + e \cos E) \, dE$$

After manipulations, the closed-form expressions for the variations of $\mathbf{h}$, $\mathbf{e}$ and a due to the atmospheric drag are obtained as:

$$\dot{\overline{\mathbf{h}}}_{drag} = -\frac{2C_0 \mu \overline{b}}{\pi \overline{a}} E(\overline{e}) \overline{\mathbf{u}}_3 \tag{7a}$$

$$\dot{\overline{\mathbf{e}}}_{drag} = -\frac{4\overline{n} \, \overline{p} C_0}{\pi \overline{e}} [K(\overline{e}) - E(\overline{e})] \overline{\mathbf{u}}_1 \tag{7b}$$

$$\dot{\overline{a}}_{drag} = -\frac{4\overline{n} \overline{a}^2 C_0}{\pi} [2K(\overline{e}) - E(\overline{e})] \tag{7c}$$

The variations due to drag of the magnitudes of vectors $\bar{\mathbf{h}}$ and $\bar{\mathbf{e}}$ are determined based on Eq. (7) as follows:

$$\dot{\bar{h}} = -\frac{2C_0\mu\bar{b}}{\pi\bar{a}}E(\bar{e}), \quad \dot{\bar{e}} = -\frac{4\bar{n}\,\bar{p}C_0}{\pi\bar{e}}[K(\bar{e}) - E(\bar{e})] \tag{8}$$

The usage of the variation of the averaged semimajor axis (namely Eq. 7c) is chosen, based on the fact that one of the equations (8) becomes redundant, since:

$$\dot{\bar{h}} = \bar{n}\left(\frac{\bar{b}}{2}\dot{\bar{a}} - \frac{\bar{e}\bar{a}^3}{\bar{b}}\dot{\bar{e}}\right)$$

(working with the average variation of the angular momentum would lead to the same results).

2.3 Satellite trajectory

Define the quantity C_u as follows:

$$C_u(\bar{a}, \bar{e}, r_{eq}, J_2) = \frac{3k_2}{2\bar{b}^3\bar{h}} = \frac{3}{4}\bar{n}J_2\left(\frac{r_{eq}}{\bar{p}}\right)^2 \tag{9}$$

where $\bar{p} = \bar{a}(1 - \bar{e}^2)$ and $\bar{n} = \mu^{1/2}\bar{a}^{-3/2}$. It is possible to offer a qualitative insight for the motion of the satellite, by taking into account the variations of the unit vectors $\bar{\mathbf{u}}_k, k = 1, 2, 3$:

$$\dot{\bar{\mathbf{u}}}_1 = C_u\left\{\left[3(\mathbf{i}_z \cdot \bar{\mathbf{u}}_3)^2 - 1\right]\bar{\mathbf{u}}_2 + 2\left[(\mathbf{i}_z \cdot \bar{\mathbf{u}}_2)(\mathbf{i}_z \cdot \bar{\mathbf{u}}_3)\right]\bar{\mathbf{u}}_3\right\} \tag{10a}$$

$$\dot{\bar{\mathbf{u}}}_2 = C_u\left\{-\left[3(\mathbf{i}_z \cdot \bar{\mathbf{u}}_3)^2 - 1\right]\bar{\mathbf{u}}_1 - 2\left[(\mathbf{i}_z \cdot \bar{\mathbf{u}}_3)(\mathbf{i}_z \cdot \bar{\mathbf{u}}_1)\right]\bar{\mathbf{u}}_3\right\} \tag{10b}$$

$$\dot{\bar{\mathbf{u}}}_3 = C_u\left\{-2\left[(\mathbf{i}_z \cdot \bar{\mathbf{u}}_2)(\mathbf{i}_z \cdot \bar{\mathbf{u}}_3)\right]\bar{\mathbf{u}}_1 + 2\left[(\mathbf{i}_z \cdot \bar{\mathbf{u}}_3)(\mathbf{i}_z \cdot \bar{\mathbf{u}}_1)\right]\bar{\mathbf{u}}_2\right\} \tag{10c}$$

The instantaneous angular $\boldsymbol{v}$ velocity of the averaged perifocal frame is deduced from:

$$\boldsymbol{v} = \frac{1}{2}\sum_{k=1}^{3}\bar{\mathbf{u}}_k \times \dot{\bar{\mathbf{u}}}_k$$

and its closed-form expression with respect to this frame is:

$$\boldsymbol{v} = C_u\left\{-2\left[(\mathbf{i}_z \cdot \bar{\mathbf{u}}_3)(\mathbf{i}_z \cdot \bar{\mathbf{u}}_1)\right]\bar{\mathbf{u}}_1 - 2\left[(\mathbf{i}_z \cdot \bar{\mathbf{u}}_2)(\mathbf{i}_z \cdot \bar{\mathbf{u}}_3)\right]\bar{\mathbf{u}}_2 + \left[3(\mathbf{i}_z \cdot \bar{\mathbf{u}}_3)^2 - 1\right]\bar{\mathbf{u}}_3\right\} \tag{11}$$

The effect of the atmospheric drag on the vector $\boldsymbol{v}$ is reflected only in the coefficient C_u, through the presence of the quantities $\bar{a}$ and $\bar{e}$, which are affected exclusively by the atmospheric drag.

Based on Eq. (11), it is possible to determine the rotation matrix $\mathbf{R}$ associated with the instantaneous angular velocity $\boldsymbol{v}$. By taking into account that:

$$\mathbf{i}_z = \sum_{k=1}^{3}(\mathbf{i}_z \cdot \bar{\mathbf{u}}_k)\bar{\mathbf{u}}_k$$

and by noticing that $\cos\bar{i} = \mathbf{i}_z \cdot \bar{\mathbf{u}}_3$, with $\bar{i}$ being the constant average orbit inclination, the vector $\boldsymbol{v}$ may be rewritten as:

$$\boldsymbol{v} = -2C_u\left\{(\cos\bar{i})\,\mathbf{i}_z + \frac{1 - 5\cos^2\bar{i}}{2}\bar{\mathbf{u}}_3\right\} \tag{12}$$

Equation ([10c](#)) may be rewritten as:

$$\dot{\bar{\mathbf{u}}}_3 = \left(-2C_u \cos \bar{i}\right) \mathbf{i}_z \times \bar{\mathbf{u}}_3 \tag{13}$$

which indicates that $\bar{\mathbf{u}}_3$ precesses about the axis defined by $\mathbf{i}_z$ with the rate $\dot{\alpha} = -2C_u \cos \bar{i}$. It follows that the closed-form expression of $\bar{\mathbf{u}}_3$ is:

$$\bar{\mathbf{u}}_3 = \mathbf{R}\left(\alpha, \mathbf{i}_z\right) \bar{\mathbf{u}}_3^0 \tag{14}$$

where $\bar{\mathbf{u}}_3^0 = \bar{\mathbf{u}}_3\left(t_0\right)$ and $\mathbf{R}\left(\alpha, \mathbf{i}_z\right)$ is defined by the Rodrigues formula [see Angeles (2002), pp. 41]:

$$\mathbf{R}\left(\alpha, \mathbf{i}_z\right) = \mathbf{I}_3 + (\sin \alpha)\,\widetilde{\mathbf{i}}_z + (1 - \cos \alpha)\,\widetilde{\mathbf{i}}_z^2, \quad \alpha = \int\limits_{t_0}^{t} \left(-2C_u \cos \bar{i}\right) \mathrm{d}t \tag{15}$$

Here $\widetilde{\mathbf{i}}_z$ denotes the skew-symmetric tensor (matrix) associated to vector $\widetilde{\mathbf{i}}_z$, satisfying $\widetilde{\mathbf{i}}_z \mathbf{x} = \widetilde{\mathbf{i}}_z \times \mathbf{x}$ for any vector $\mathbf{x}$.

The expression of the instantaneous angular velocity $\boldsymbol{\upsilon}$ may be rewritten as:

$$\boldsymbol{\upsilon} = \dot{\alpha}\mathbf{i}_z + \mathbf{R}\left(\alpha, \mathbf{i}_z\right) \left[C_u \left(5 \cos^2 \bar{i} - 1\right) \bar{\mathbf{u}}_3^0\right] \tag{16}$$

It is easy now to verify that the rotation matrix

$$\mathbf{R} = \mathbf{R}\left(\alpha, \mathbf{i}_z\right) \mathbf{R}\left(\gamma, \bar{\mathbf{u}}_3^0\right), \quad \gamma = \int\limits_{t_0}^{t} C_u \left(5 \cos^2 \bar{i} - 1\right) \mathrm{d}t \tag{17}$$

satisfies $\dot{\mathbf{R}} = \widetilde{\boldsymbol{\upsilon}}\mathbf{R}$, $\mathbf{R}\left(t_0\right) = \mathbf{I}_3$, and therefore it is the rotation matrix associated with the instantaneous angular velocity $\boldsymbol{\upsilon}$.

The motion may now be visualized as follows: At the initial moment $t = t_0$, a plane Π having the normal $\bar{\mathbf{u}}_3^0 = \bar{\mathbf{h}}_0 \times \bar{\mathbf{e}}_0 / \left(\left\|\bar{\mathbf{h}}_0\right\| \left\|\bar{\mathbf{e}}_0\right\|\right)$ is formed. The plane Π starts rotating about its own normal with the rate $\dot{\gamma} = C_u \left(5 \cos^2 \bar{i} - 1\right)$, while its normal is precessing about the $\mathbf{i}_z$ vector with the rate $\dot{\alpha} = -2C_u \cos \bar{i}$. The satellite moves in the rotating plane Π on a "shrinking" ellipse, which suffers from a semimajor axis decay with the rate $\dot{\bar{a}} < 0$, given in Eq. ([7c](#)), and a "circularization", modeled by the decrease in the eccentricity, expressed in Eq. ([8](#)). The motion on this shrinking ellipse is detailed in the next section.

A way to emphasize the aforementioned "circularization" of the ellipse is to compare the rates of decrease of the semimajor axis $\bar{a}$ and the semiminor axis $\bar{b}$ of the ellipse. After some computations, it is obtained:

$$\frac{\dot{\bar{b}}}{\sqrt{1 - \bar{e}^2}} - \dot{\bar{a}} = \frac{4C_0 \sqrt{\mu \bar{a}}}{\pi} \left[K\left(\bar{e}\right) - E\left(\bar{e}\right)\right] < 0$$

which leads to:

$$\dot{\bar{b}} < \dot{\bar{a}}\sqrt{1 - \bar{e}^2} < \dot{\bar{a}} \tag{18}$$

The interpretations of Eq. ([18](#)) is that the rate of decrease of the semimajor axis is faster than that of the semiminor axis, and therefore the use of term "circularization" is legitimate.

Note that the two aforementioned rotations recover the already known variational equations for the averaged right ascension of the ascending node $\overline{\Omega}$ and for the averaged argument of perigee $\overline{\omega}$:

$$\dot{\overline{\Omega}} = \dot{\alpha}, \quad \dot{\overline{\omega}} = \dot{\gamma}$$

which become the well-known initial value problems [see Battin (1999), pp. 504, Schaub and Junkins (2003), pp. 408]:

$$\dot{\overline{\Omega}} = -\frac{3}{2} J_2 \overline{n} \left(\frac{r_{eq}}{\overline{p}}\right)^2 \cos \overline{i}, \quad \overline{\Omega}(t_0) = \overline{\Omega}_0 \quad \dot{\overline{\omega}} = \frac{3}{4} J_2 \overline{n} \left(\frac{r_{eq}}{\overline{p}}\right)^2 \left(5 \cos^2 \overline{i} - 1\right), \quad \overline{\omega}(t_0) = \overline{\omega}_0$$

(19)

Remark that $\overline{\Omega}$ and $\overline{\omega}$ are no longer varying linearly with time, due to the fact that the quantities $\overline{n}$ and $\overline{p}$ are not constant, given the presence of the atmospheric drag. The solution to the initial value problems (19) will be addressed in the next sections.

2.4 Satellite motion on the trajectory

The considerations made in the previous section have concerned the global behaviour of the motion, without any reference to the specific motion on the trajectory. For this purpose, the variational equation for one of the anomalies (true, eccentric or mean) is required:

$$\frac{d}{dt}() = \frac{\partial}{\partial t}() + \left[\frac{\partial}{\partial \dot{\mathbf{r}}}()\right] \cdot \mathbf{f}_d$$

where $()$ is any of the anomalies f, E or M [see Battin (1999), pp. 501–503]. The *mean anomaly M* will be subjected to the averaging procedure, since it contains the sixth constant of the unperturbed motion, related to the time of periapsis passage t_P.

By taking into account the closed-form expressions which are obtained in the right-hand side of the equalities above, it follows that [see Battin (1999), pp. 502–503]:

$$\dot{M} = n + \frac{rb}{ha^2 e} \left[\cos f \left(\mathbf{r} \cdot \mathbf{f}_d\right) - \frac{a}{h}(r + p) \sin f \left(\dot{\mathbf{r}} \cdot \mathbf{f}_d\right)\right]$$

(20)

At this point it is more natural to perform the computations in the Local-Vertical-Local-Horizontal (LVLH) frame of the satellite, defined by the orthogonal unit vectors:

$$\mathbf{i}_1 = \hat{\mathbf{r}}; \quad \mathbf{i}_2 = \hat{\mathbf{h}} \times \hat{\mathbf{r}}; \quad \mathbf{i}_3 = \hat{\mathbf{h}}$$

where the perturbing accelerations have the expressions:

$$\mathbf{f}_{J_2}^{LVLH} = -\frac{3k_2}{r^4} \begin{bmatrix} 1 - 3\sin^2 i \sin^2(\omega + f) \\ \sin^2 i \sin^2(2\omega + 2f) \\ \sin(2i) \sin(\omega + f) \end{bmatrix}, \quad \mathbf{f}_{drag}^{LVLH} = -C_0 \|\mathbf{v}\| \frac{h}{p} \begin{bmatrix} e \sin f \\ p/r \\ 0 \end{bmatrix}$$

Equation (20) transforms into [see Battin (1999), pp. 488]:

$$\dot{M} = n + \frac{b}{hae} \left[(p \cos f - 2re) f_{dr} - \sin f (p + r) f_{d\theta}\right]$$

where f_{dr} is the component of the perturbing acceleration along the $\mathbf{i}_1$ unit vector of the LVLH frame, while $f_{d\theta}$ is the component along the $\mathbf{i}_2$ unit vector of the same frame. Averaging over one period of the unperturbed motion provides the following expression:

$$\dot{\overline{M}} = \overline{n} + C_u \sqrt{1 - \overline{e}^2} \left(3 \cos^2 \overline{i} - 1\right)$$

(21)

The classic differential equation for the averaged *mean anomaly* is recovered in this way, with the same remark that the quantity in the right-hand side of Eq. (21) is not a constant, due to the fact that both $\overline{a}$ and $\overline{e}$ are subject to variations, because of the presence of the atmospheric drag.

For an observer whose world is shrinking together with the instantaneous ellipse, the averaged motion of the satellite is Keplerian on this ellipse, with a gravitational parameter

which depends both on the shape of the ellipse and on the orbit inclination. The value of this fictitious gravitational parameter is:

$$\overline{\mu}^* = \mu \left[1 + \frac{C_u \overline{b}}{\overline{n}\overline{a}} \left(3 \cos^2 \overline{i} - 1 \right) \right]^2 \tag{22}$$

The rate of variation of the fictitious gravitational parameter $\overline{\mu}^*$ is determined to be:

$$\dot{\overline{\mu}}^* = 12 C_0 k_2 \frac{\overline{n}\overline{a}^2}{\overline{b}^3} \left[1 + \frac{C_u \overline{b}}{\overline{n}\overline{a}} \left(3 \cos^2 \overline{i} - 1 \right) \right] \left[K\left(\overline{e}\right) + E\left(\overline{e}\right) \right] > 0 \tag{23}$$

3 Analytic solutions

Eventually, the initial value problems which model the motion of the satellite under the influence of J_2 and the atmospheric drag is

$$\dot{\overline{a}} = -4 C_0 \overline{n}\overline{a}^2 \frac{2K\left(\overline{e}\right) - E\left(\overline{e}\right)}{\pi} \tag{24a}$$

$$\dot{\overline{e}} = -4 C_0 \overline{n}\,\overline{p} \frac{\left[K\left(\overline{e}\right) - E\left(\overline{e}\right) \right]}{\pi \overline{e}} \tag{24b}$$

$$\dot{\overline{i}} = 0 \tag{24c}$$

$$\dot{\overline{M}} = \overline{n} + \frac{C_u \overline{b}}{\overline{a}} \sqrt{1 - \overline{e}^2} \left(3c^2 - 1 \right) \tag{24d}$$

$$\dot{\overline{\omega}} = C_u \left(5c^2 - 1 \right) \tag{24e}$$

$$\dot{\overline{\Omega}} = -2 C_u c$$

$$\overline{a}\left(t_0\right) = \overline{a}_0, \ \overline{e}\left(t_0\right) = \overline{e}_0, \ \overline{i}\left(t_0\right) = \overline{i}_0, \quad \overline{M}\left(t_0\right) = \overline{M}_0, \quad \overline{\omega}\left(t_0\right) = \overline{\omega}_0, \quad \overline{\Omega}\left(t_0\right) = \overline{\Omega}_0 \tag{24f}$$

where $c = \cos \overline{i}$. It is obvious now that Eqs. (24a) and (24b) need to be solved first, since the quantities $\overline{a}$ and $\overline{e}$ are involved in all the other equations.

3.1 The case of small eccentricity ($e^4 \simeq 0$)

In order to obtain an analytic solution to Eq. (24), Taylor series expansions with respect to the averaged eccentricity $\overline{e}$ are performed, together with the introduction of a new independent variable τ, defined by:

$$dt = \frac{d\tau}{B\left(\overline{a}, \overline{e}\right)}, \quad \tau\left(t_0\right) = \overline{a}_0 \tag{25}$$

where the expression of $B\left(\overline{a}, \overline{e}\right)$ is:

$$B\left(\overline{a}, \overline{e}\right) = -\frac{C_0 \overline{n}\overline{a}^2}{2} \left(4 + 3\overline{e}^2 \right) \tag{26}$$

A new system of differential equations will emerge, where the derivatives, denoted with $(\ )'$, are computed with respect to the new independent variable τ as follows

$$(\ )' = \frac{d}{d\tau} (\ ) = \frac{1}{B\left(\overline{a}, \overline{e}\right)} \frac{d}{dt} (\ )$$

A new differential equation, which links the time variable t to the independent variable τ (similar to Kepler's equation in the unperturbed case), will be derived and solved explicitly in each situation.

Since the averaged inclination remains constant, its differential equation will be omitted. Equations (24) are rewritten as:

$$\bar{a}' = -4C_0\sqrt{\mu}\bar{a}\frac{2K(\bar{e}) - E(\bar{e})}{\pi B(\bar{a}, \bar{e})} \tag{27a}$$

$$\bar{e}' = -\frac{4C_0\sqrt{\mu}}{\sqrt{\bar{a}}}\frac{(1-\bar{e}^2)[K(\bar{e}) - E(\bar{e})]}{\pi \bar{e} B(\bar{a}, \bar{e})} \tag{27b}$$

$$\overline{M}' = \frac{\bar{n}}{B(\bar{a}, \bar{e})} + \frac{C_u\sqrt{1-\bar{e}^2}(3c^2 - 1)}{B(\bar{a}, \bar{e})} \tag{27c}$$

$$\bar{\omega}' = \frac{C_u(5c^2 - 1)}{B(\bar{a}, \bar{e})} \tag{27d}$$

$$\overline{\Omega}' = -\frac{2C_u c}{B(\bar{a}, \bar{e})} \tag{27e}$$

$$t' = \frac{1}{B(\bar{a}, \bar{e})} \tag{27f}$$

After expanding the right-hand sides of Eq. (27a–27e) in Taylor series and assuming that $\mathcal{O}(\bar{e}^4) = 0$, the system becomes:

$$\bar{a}' = 1 \tag{28a}$$

$$\bar{e}' = \frac{\bar{e}}{2\bar{a}} \tag{28b}$$

$$\overline{M}' = -\frac{1}{8C_0}\frac{4 - 3\bar{e}^2}{\bar{a}^2} - \frac{3k_2(3c^2 - 1)}{16\mu C_0}\frac{(4 + 3\bar{e}^2)}{\bar{a}^4} \tag{28c}$$

$$\bar{\omega}' = -\frac{3k_2(5c^2 - 1)}{16\mu C_0}\frac{(4 + 5\bar{e}^2)}{\bar{a}^4} \tag{28d}$$

$$\overline{\Omega}' = \frac{3k_2 c}{8\mu C_0}\frac{(4 + 5\bar{e}^2)}{\bar{a}^4} \tag{28e}$$

$$t' = -\frac{2}{C_0\sqrt{\mu}}\frac{1}{\sqrt{\bar{a}}(4 + 3\bar{e}^2)} \tag{28f}$$

The solutions to Eq. (28a) and (28b) are:

$$\bar{a} = \tau \tag{29a}$$

$$\bar{e} = \alpha_0\sqrt{\tau}, \quad \alpha_0 = \frac{\bar{e}_0}{\sqrt{\bar{a}_0}} \tag{29b}$$

From Eq. (28f), the time-explicit expression of the averaged semimajor axis may now be obtained:

$$\beta_0 = \frac{\sqrt{3}}{2}\bar{e}_0$$

$$\bar{a} = \frac{\bar{a}_0}{\beta_0^2}\tan^2[\arctan(\beta_0) - \beta_0\bar{n}_0\bar{a}_0 C_0(t - t_0)] \tag{30}$$

The rest of the differential equations are solved by simple integration, yielding:

$$\bar{e} = \frac{2}{\sqrt{3}} \tan\left[\arctan(\beta_0) - \beta_0 \bar{n}_0 \bar{a}_0 C_0 (t - t_0)\right] \tag{31a}$$

$$\bar{M} - \bar{M}_0 = \frac{1}{8} \frac{1}{C_0} \left[\frac{4}{\tau} + 3\alpha_0^2 \ln\frac{\tau}{\bar{a}_0}\right]\Bigg|_{\tau=\bar{a}_0}^{\tau=\bar{a}} + \frac{3k_2\left(3c^2 - 1\right)}{16\mu} \frac{1}{C_0} \left[\frac{3\alpha_0^2}{2}\frac{1}{\tau^2} + \frac{4}{3\tau^3}\right]\Bigg|_{\tau=\bar{a}_0}^{\tau=\bar{a}} \tag{31b}$$

$$\bar{\omega} - \bar{\omega}_0 = \frac{3k_2\left(5c^2 - 1\right)}{16\mu} \frac{1}{C_0} \left[\frac{5\alpha_0^2}{2}\frac{1}{\tau^2} + \frac{4}{3\tau^3}\right]\Bigg|_{\tau=\bar{a}_0}^{\tau=\bar{a}} \tag{31c}$$

$$\bar{\Omega} - \bar{\Omega}_0 = -\frac{3k_2 c}{8\mu} \frac{1}{C_0} \left[\frac{5\alpha_0^2}{2}\frac{1}{\tau^2} + \frac{4}{3\tau^3}\right]\Bigg|_{\tau=\bar{a}_0}^{\tau=\bar{a}} \tag{31d}$$

In order to avoid the singularities induced by the choice of classic orbital elements, the equations of motion may be written with respect to the equinoctial variables $\left(\bar{a}, \bar{P}_1, \bar{P}_2, \bar{Q}_1, \bar{Q}_2, \bar{\sigma}\right)$ as follows:

$$\bar{a} = \frac{\bar{a}_0}{\beta_0^2} \tan^2\left[\arctan\beta_0 - \beta_0 \bar{n}_0 \bar{a}_0 C_0 (t - t_0)\right] \tag{32a}$$

$$\bar{P}_1 = \frac{2}{\sqrt{3}} \tan\left[\arctan\beta_0 - \beta_0 \bar{n}_0 \bar{a}_0 C_0 (t - t_0)\right] \sin\bar{\omega} \tag{32b}$$

$$\bar{P}_2 = \frac{2}{\sqrt{3}} \tan\left[\arctan\beta_0 - \beta_0 \bar{n}_0 \bar{a}_0 C_0 (t - t_0)\right] \cos\bar{\omega} \tag{32c}$$

$$\bar{Q}_1 = \bar{u}_0 \sin\left\{\arctan\frac{\bar{Q}_1(t_0)}{\bar{Q}_2(t_0)} - \frac{3k_2 c}{8\mu} \frac{1}{C_0} \left[\frac{5\alpha_0^2}{2}\frac{1}{\tau^2} + \frac{4}{3\tau^3}\right]\Bigg|_{\tau=\bar{a}_0}^{\tau=\bar{a}}\right\} \tag{32d}$$

$$\bar{Q}_2 = \bar{u}_0 \cos\left\{\arctan\frac{\bar{Q}_1(t_0)}{\bar{Q}_2(t_0)} - \frac{3k_2 c}{8\mu} \frac{1}{C_0} \left[\frac{5\alpha_0^2}{2}\frac{1}{\tau^2} + \frac{4}{3\tau^3}\right]\Bigg|_{\tau=\bar{a}_0}^{\tau=\bar{a}}\right\} \tag{32e}$$

$$\bar{\sigma} = \bar{\sigma}_0 + \frac{1}{8C_0} \left[\frac{4}{\tau} + 3\alpha_0^2 \ln\frac{\tau}{\bar{a}_0}\right]\Bigg|_{\tau=\bar{a}_0}^{\tau=\bar{a}} +$$

$$\frac{k_2}{16\mu C_0} \left[\frac{3\alpha_0^2\left(17c^2 - 5c - 4\right)}{\tau^2} + \frac{8\left(4c^2 - c - 1\right)}{\tau^3}\right]\Bigg|_{\tau=\bar{a}_0}^{\tau=\bar{a}} \tag{32f}$$

where:

$$\alpha_0 = \frac{\sqrt{\bar{P}_1^2(t_0) + \bar{P}_2^2(t_0)}}{\sqrt{\bar{a}_0}} \tag{33a}$$

$$\beta_0 = \frac{\sqrt{3}}{2} \alpha_0 \sqrt{\bar{a}_0} \tag{33b}$$

$$\bar{u}_0 = \sqrt{\bar{Q}_1^2(t_0) + \bar{Q}_2^2(t_0)}; \tag{33c}$$

$$\bar{\omega}_0 = \arctan\frac{\bar{P}_1(t_0)}{\bar{P}_2(t_0)}; \tag{33d}$$

$$\overline{\sigma}_0 = \overline{\varpi}_0 + \overline{M}_0; \tag{33e}$$

$$\varpi = \overline{\varpi}_0 + \frac{k_2 \left(5c^2 - 2c - 1\right)}{32\mu C_0} \left[\frac{15\alpha_0^2}{\tau^2} + \frac{8}{\tau^3} \right]_{\tau=\overline{a}_0}^{\tau=\overline{a}} \tag{33f}$$

The presence of C_0 at the denominator in Eqs. (31) might seem to introduce a singularity. However, it is only apparent, due to the fact that expressions of the type $(\overline{a} - \overline{a}_0) \, g \, (\overline{a}, \overline{a}_0)$, $g \, (\overline{a}, \overline{a}_0) \neq 0$, are present at the numerators. By taking into account Eq. (30), it follows that:

$$\lim_{C_0 \to 0} \frac{\overline{a} - \overline{a}_0}{C_0} = -2\overline{n}_0 \overline{a}_0^2 \left(1 + \beta_0^2\right) (t - t_0) \tag{34}$$

If the limit $C_0 \to 0$ is made in Eq. (31), the classic averaged variational equations for J_2 only are obtained, after some manipulations. The singularity is therefore removed. For numerical purposes, in order to avoid the inconvenience of C_0 being small, the series expansion of the difference $\overline{a} - \overline{a}_0$ in powers of C_0 is considered, which is deduced based on Eq. (30) as:

$$\overline{a} - \overline{a}_0 = \overline{a}_0 \left(1 + \beta_0^2\right) \sum_{k=1}^{\infty} [\overline{n}_0 \overline{a}_0 C_0 \, (t - t_0)]^k \, d_k \tag{35}$$

where the first relevant values of the coefficients d_k are:

$$d_1 = -2$$
$$d_2 = 1 + 3\beta_0^2$$
$$d_3 = -\frac{4}{3}\beta_0^2 \left(2 + 3\beta_0^2\right)$$
$$d_4 = \frac{1}{3}\beta_0^2 \left(15\beta_0^4 + 15\beta_0^2 + 2\right)$$
$$d_5 = -\frac{2}{15}\beta_0^2 \left(45\beta_0^4 + 60\beta_0^2 + 17\right)$$

For the logarithmic term which is present in the expression of $\overline{M}$, in Eq. (31b), the following series expansion

$$\frac{1}{C_0} \ln \frac{\overline{a}}{\overline{a}_0} = \overline{n}_0 \overline{a}_0 \left(1 + \beta_0^2\right) (t - t_0) \sum_{k=1}^{\infty} [\overline{n}_0 \overline{a}_0 C_0 \, (t - t_0)]^k \, g_k \tag{36}$$

should be used, where the first relevant values of the coefficients g_k are:

$$g_1 = -2$$
$$g_2 = -1 + \beta_0^2$$
$$g_3 = -\frac{2}{3} \left(1 + \beta_0^4\right)$$
$$g_4 = \frac{1}{6} \left(1 - \beta_0^2\right) \left(3\beta_0^4 + 4\beta_0^2 + 3\right)$$
$$g_5 = -\frac{2}{15}\beta_0^2 \left(3\beta_0^8 + 2\beta_0^6 + 2\beta_0^2 + 3\right)$$

3.2 The case of very small eccentricity ($\overline{e}^2 \simeq 0$)

Simpler expressions may be obtained if a more restrictive assumption is made, namely that the eccentricity is such that $\mathcal{O} \left(\overline{e}_0^2\right) = 0$. By expanding in Taylor series in Eqs. (30) and (31),

it follows that:

$$\bar{a} = \bar{a}_0 - 2C_0\sqrt{\mu}\,(t-t_0)\,\sqrt{\bar{a}_0} + \mu C_0^2\,(t-t_0)^2\,\bar{a}_0 + \mathcal{O}\left(\bar{e}_0^2\right)$$

$$\bar{e} = \left[1 - \frac{C_0\sqrt{\mu}}{\sqrt{\bar{a}_0}}\,(t-t_0)\right]\bar{e}_0 + \mathcal{O}\left(\bar{e}_0^3\right)$$

The analytic solution is expressed as follows:

$$\bar{a} = \bar{a}_0\left[1 - C_0\bar{n}_0\bar{a}_0\,(t-t_0)\right]^2 \tag{37a}$$

$$\bar{e} = \alpha_0\sqrt{\bar{a}} \tag{37b}$$

$$\overline{M} - \overline{M}_0 = \frac{1}{2C_0}\left(\frac{1}{\bar{a}} - \frac{1}{\bar{a}_0}\right) + \frac{k_2\left(3c^2 - 1\right)}{4\mu C_0}\left(\frac{1}{\bar{a}^3} - \frac{1}{\bar{a}_0^3}\right) \tag{37c}$$

$$\bar{\omega} - \bar{\omega}_0 = \frac{k_2\left(5c^2 - 1\right)}{4\mu C_0}\left(\frac{1}{\bar{a}^3} - \frac{1}{\bar{a}_0^3}\right) \tag{37d}$$

$$\overline{\Omega} - \overline{\Omega}_0 = -\frac{k_2 c}{2\mu C_0}\left(\frac{1}{\bar{a}^3} - \frac{1}{\bar{a}_0^3}\right) \tag{37e}$$

The inconvenience of having C_0 at the denominator is removed by taking into account Eq. (37a):

$$\frac{1}{C_0}\left(\frac{1}{\bar{a}} - \frac{1}{\bar{a}_0}\right) = \frac{\sqrt{\mu}\left(\sqrt{\bar{a}_0} + \sqrt{\bar{a}}\right)}{\bar{a}_0\bar{a}}\,(t-t_0) \tag{38a}$$

$$\frac{1}{C_0}\left(\frac{1}{\bar{a}^3} - \frac{1}{\bar{a}_0^3}\right) = \frac{\sqrt{\mu}\left(\bar{a}_0^2 + \bar{a}\bar{a}_0 + \bar{a}^2\right)\left(\sqrt{\bar{a}_0} + \sqrt{\bar{a}}\right)}{\bar{a}_0^3\bar{a}^3}\,(t-t_0) \tag{38b}$$

The singularities which occur at low inclinations and small eccentricities are removed by using equinoctial elements, instead of the classic ones. By using also Eqs. (36), Eqs. (37) are rewritten as:

$$\overline{P}_1 = \alpha_0\left[1 - C_0\bar{n}_0\bar{a}_0\,(t-t_0)\right]\sin\bar{\omega} \tag{39a}$$

$$\overline{P}_2 = \alpha_0\left[1 - C_0\bar{n}_0\bar{a}_0\,(t-t_0)\right]\cos\bar{\omega} \tag{39b}$$

$$\overline{Q}_1 = \bar{u}_0\sin\left[\arctan\frac{\overline{Q}_1(t_0)}{\overline{Q}_2(t_0)} - \frac{k_2 c}{2\mu C_0}\left(\frac{1}{\bar{a}^3} - \frac{1}{\bar{a}_0^3}\right)\right] \tag{39c}$$
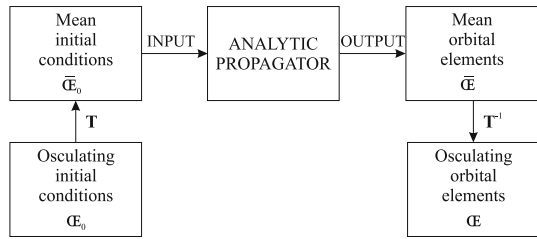
$$\overline{Q}_2 = \bar{u}_0\cos\left[\arctan\frac{\overline{Q}_1(t_0)}{\overline{Q}_2(t_0)} - \frac{k_2 c}{2\mu C_0}\left(\frac{1}{\bar{a}^3} - \frac{1}{\bar{a}_0^3}\right)\right] \tag{39d}$$

$$\bar{\sigma} = \bar{\sigma}_0 + \frac{\sqrt{\mu}\left(\sqrt{\bar{a}_0} + \sqrt{\bar{a}}\right)}{2\bar{a}_0\bar{a}}\left[1 - \frac{k_2\left(-4c^2 + c + 1\right)}{\mu}\frac{\left(\bar{a}_0^2 + \bar{a}\bar{a}_0 + \bar{a}^2\right)}{\bar{a}_0^2\bar{a}^2}\right](t-t_0) \tag{39e}$$

where are $\bar{u}_0$, $\bar{\omega}_0$, $\bar{\sigma}_0$ are defined in Eqs. (33) and

$$\bar{\omega} = \bar{\omega}_0 - \frac{k_2\left(-5c^2 + 2c + 1\right)}{4\sqrt{\mu}\bar{a}_0^3\bar{a}^3}\left(\bar{a}_0^2 + \bar{a}\bar{a}_0 + \bar{a}^2\right)\left(\sqrt{\bar{a}_0} + \sqrt{\bar{a}}\right)(t-t_0) \tag{40}$$

Fig. 1 Proposed orbit
propagation algorithm

4 Algorithm for orbit propagation

The time-explicit solutions obtained in the previous section describe the averaged motion under the influence of J_2 and atmospheric drag. However, the set of averaged orbital elements does not belong to the space of osculating orbital elements, which describe the real motion of the satellite. A mapping between these two sets of elements therefore needs to be established via a so-called *contact transformation*.

Because we target short-term orbit predictions in this study, we assume that the effects of the atmospheric drag may be locally ignored in the contact transformation. This assumption allows us to exploit the classic canonical theory for Hamiltonian systems for transforming osculating elements into mean elements and vice versa. Since the eccentricities considered herein are small, a slightly-modified version of the canonical contact transformation developed in Brouwer (1959) is used. The transformation was originally developed by Lyddane (1963), and the governing equations can be found in Schaub and Junkins (2003), Appendix G.

The orbit propagation is performed as presented in Fig. 1. At the initial epoch $t = t_0$, the input consists of the osculating equinoctial elements $\boldsymbol{Œ}_0 = \left(a_0, P_{1,0}, P_{2,0}, Q_{1,0}, Q_{2,0}, \sigma_0\right)$. The osculating to mean transformation is applied to these coordinates:

$$\boldsymbol{Œ}_0 \xrightarrow{\ \mathbf{T}\ } \overline{\boldsymbol{Œ}}_0$$

in order to obtain the mean initial conditions $\overline{\boldsymbol{Œ}}_0 = \left(\overline{a}_0, \overline{P}_{1,0}, \overline{P}_{2,0}, \overline{Q}_{1,0}, \overline{Q}_{2,0}, \overline{\sigma}_0\right)$. The equations derived in Section 3 are used to propagate the averaged orbital elements, starting from $\overline{\boldsymbol{Œ}}_0$. At each step of the propagation, the inverse contact transformation is applied in order to recover the osculating orbital elements:

$$\overline{\boldsymbol{Œ}}(t) \xrightarrow{\ \mathbf{T}^{-1}\ } \boldsymbol{Œ}(t)$$

which constitute the output of the propagation.

5 Validation of the analytic propagator

5.1 Deterministic simulations

Our analytic propagator is demonstrated using a nanosatellite ($C_D = 2.2$, $S_{ref}/m = 0.01$ m^2/kg) in a quasi-circular orbit ($e_0 = 0.001$, $i = 51°$, $f_0 = 20°$, $\omega_0 = 0°$, $\Omega_0 = 0°$). The simulations were performed for a time interval of 2 days and for two initial altitudes, namely 350 and 600 km. The predictive capability of the propagator for very small eccentricities ($e^2 \simeq 0$) was assessed through comparison with direct numerical integration of the equations

Fig. 2 *Dashed red line*
numerical propagation with
J_2-only, solid blue: analytic
propagation with Drag+J_2. **a**
Error in position for an initial
altitude of 350 km ($\rho_0 = 10^{-11}$
kg/m^3). **b** Error in position for an
initial altitude of 600 km
($\rho_0 = 10^{-13}$ kg/m^3). **c** Error in
position between numerical and
analytic propagations with no
drag for an initial altitude of
350 km
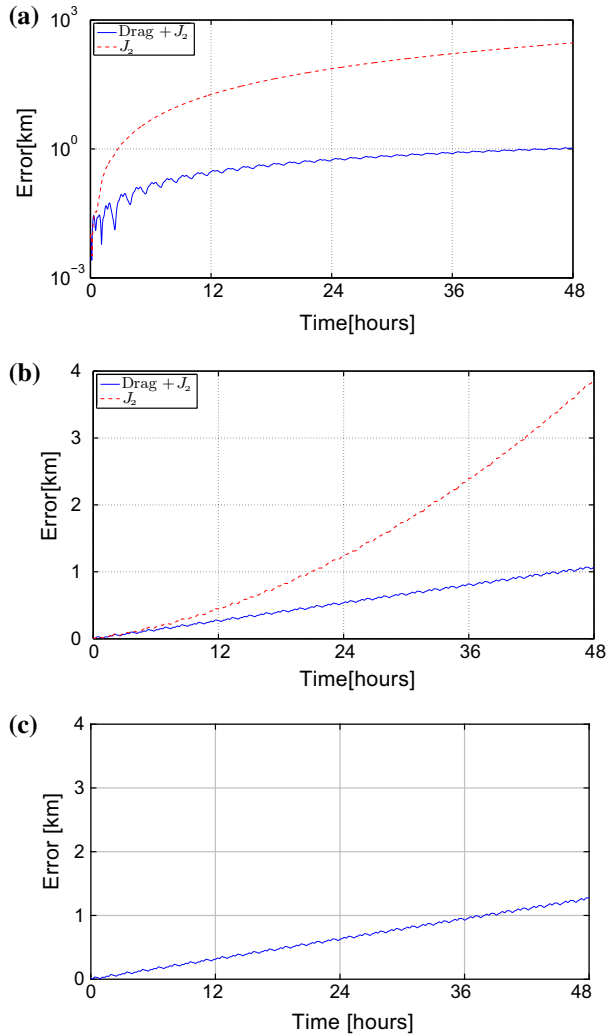
of motion. Similar results were achieved using the propagator for small eccentricities ($e^4 \simeq$
0), which is therefore not considered in this section.

   Figure 2a, b compare the outcome of three different propagations, i.e., numerical prop-
agation with Drag+J_2, numerical propagation with J_2-only, and analytic propagation with
Drag+J_2 at 350 and 600 km, respectively. Figure 2a shows that neglecting drag in the numer-
ical propagation at 350 km can result in a position error of the order of several hundreds
kilometers. The error with the analytic propagator drops down to approximately 1 km, which
represents the evidence of the good predictive capability and usefulness of the proposed time-
explicit solution. Interestingly, the error made by the analytic propagator is also around 1 km
at an altitude of 600 km, as displayed in Fig. 2b. Considering that drag is much smaller at this
altitude, this result suggests that the error is mainly inherited from the Earth's oblateness,
i.e. from the averaging of the J_2 effect and the absence of drag in the contact transformation.
Further confirmation of this finding is obtained by setting the atmospheric density to 0 in the
simulations, as in Fig. 2c, which also gives an error of 1 km.

In addition, the fact that the error of the analytic propagator evolves nearly linearly and with non-zero initial slope is another indication that the drift is due to the Earth's oblateness. Small errors in the initial mean estimation due to the first-order contact transformation are mapped into errors in the coefficient C_u in Eq. (9), which, in turn, modifies the mean orbital period and results in a linear drift of the mean anomaly.

5.2 Statistical analysis

In view of the important uncertainty affecting atmospheric drag and because the considered contact transformation neglects drag, a statistical validation of the analytic propagator was also performed. The atmospheric density ρ was chosen according to the Harris–Priester model for a given altitude H as follows. Consider $\rho_{nom}(H)$ the deterministic component of the density, computed as the mean between the minimum and maximum values of the density of the Harris–Priester model at altitude H. The quantity C_ρ is a random variable ranging from -1 to 1, and it is used to correct the density, i.e., $\rho(H, C_\rho) = \rho_{nom}(H) \cdot 10^{C_\rho}$. Figure 3 depicts the dependence of the density with the altitude obtained through this process. The initial Keplerian elements were also modeled as uniformly distributed random variables with the lower and upper bounds given in Table 1.

Two different simulations are compared by means of Monte-Carlo propagation of 20000 samples of the stochastic input variables. Specifically, the difference between analytic (i.e., Brouwer's model) and numerical propagations for J_2-only is compared against the difference between analytic and numerical propagations in the Drag+J_2 case. Figure 4a depicts the resulting median errors in position, as well as the 90 % confidence bounds. The differences between the two errors are negligible, since the two medians are almost overlapping. In

Fig. 3 Density profile in function of the altitude. The solid line is the the mean between the minimum and maximum values of the density of the Harris–Priester model at a given altitude. The shaded region indicates the variability introduced by the parameter C_ρ
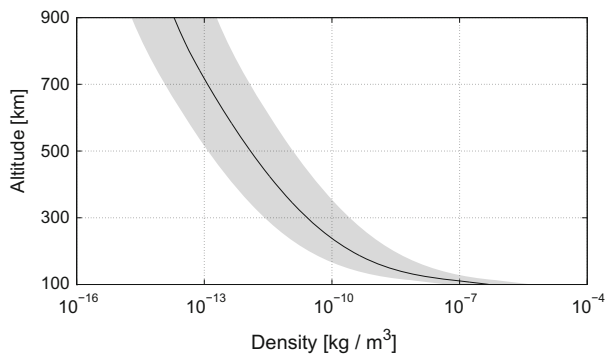
Table 1 Lower and upper bounds of the Keplerian elements used in the Monte Carlo simulations

Variable	Lower bound	Upper bound	Description
H_0	300 km	800 km	Geocentric altitude
e_0	0	$5 \cdot 10^{-3}$	Eccentricity
i_0	0°	180°	Inclination
ω_0	0°	360°	Argument of perigee
Ω_0	0°	360°	RAAN
f_0	0°	360°	True anomaly

Fig. 4 Medians and 90 % confidence bounds for the error after 2 days for the J_2 & drag and J_2-only analytic propagators. **a** With respect to time. **b** With respect to the initial altitude H_0
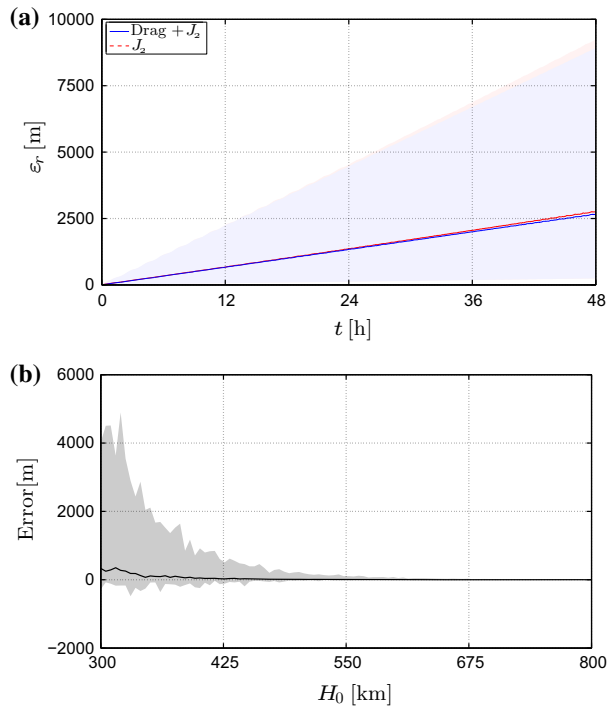
addition, the correlation between the position errors of the drag+J_2 and the J_2 -only analytic propagators is 99.8 %, thus showing that *the main contribution to the error is the J_2 effect.*

Figure 4b depicts the error between the two analytic propagators (J_2 & drag and J_2-only) as a function of the initial altitude of the satellite. As expected, the 90 % confidence bounds are converging to 0 when altitude increases, while the median value always remains very close to 0.

6 Conclusions

A new time-explicit solution for the motion of a satellite in the atmosphere of an oblate planet was proposed in this paper. The solution was developed in two cases, namely small and very small initial osculating eccentricities. The resulting analytic propagator was validated using deterministic and stochastic numerical simulations, which evidenced that the propagation errors are mostly inherited from Brouwer's first-order model, through the truncation of the Fourier series of the J_2 potential, and, to a lesser extent, from the Brouwer–Lyddane contact transformation. The propagator is able to run on a processor with very limited power capabilities, such as those onboard satellites.

Future research will generalize this analytic solution to more advanced atmospheric models, e.g., accounting for the vertical exponential rarefaction of the atmosphere. The possibility of adapting higher-order contact transformations such that they can account for atmospheric drag will also be investigated.

References

Abramowitz, M., Stegun, I.A.: Handbook of Mathematical Functions with Formulas, Graphs, and Mathematical Tables. Dover, New York (1964)

Angeles, J.: Fundamentals of Robotic Mechanical Systems. Springer, New York (2002)

Battin, R.H.: An Introduction to the Mathematics and Methods of Astrodynamics. AIAA, Reston (1999)

Brouwer, D.: Solution of the problem of artificial satellite theory without drag. Astron. J. **64**, 378 (1959)

Brouwer, D., Hori, G.-I.: Theoretical evaluation of atmospheric drag effects in the motion of an artificial satellite. Astron. J. **66**, 193 (1961)

Cain, B.J.: Determination of mean elements for Brouwer's satellite theory. Astron. J. **67**, 391 (1962)

Chao, C.C.: Applied Orbit Perturbation and Maintenance. Aerospace Press, New York (2005)

Cid, R., Lahulla, J.F.: Perturbaciones de corto periodo en el movimiento de un satélite artificial, en función de las variables de Hill. Publicaciones de la Revista de la Academia de Ciencias de Zaragoza **24**, 159–165 (1969)

Condurache, D., Martinusi, V.: Analytical orbit propagator based on vectorial orbital elements. In AIAA Guidance, Navigation and Control Conference, Boston, MA, Aug 2013

Dell'Elce, L., Kerschen, G.: Probabilistic assessment of the lifetime of low-earth-orbit spacecraft: uncertainty characterization. J. Guid Control Dyna **1**, 1–13 (2014)

Deprit, A.: Canonical transformations depending on a small parameter. Celest. Mech. **1**, 12–30 (1969)

Deprit, A.: The elimination of the Parallax in satellite theory. Celest. Mech. **24**, 111–153 (1981)

Franco, J.M.: An analytic solution for Deprit's radial intermediary with drag in the equatorial case. Bull. Astron. Inst. Czechoslov. **42**, 219–224 (1991)

Garfinkel, B.: The orbit of a satellite of an oblate planet. Astron. J. **64**, 353 (1959)

Gurfil, P., Lara, M.: Satellite onboard orbit propagation using Déprits radial intermediary. Celest. Mech. Dyn. Astron. **120**(2), 217–232 (2014)

Hestenes, D.: New Foundations for Classical Mechanics. Kluwer Academic Publishers, New York (1999)

King-Hele, D.: Butterworths mathematical texts. In: Theory of Satellite Orbits in an Atmosphere. Butterworths, New York (1964)

Kozai, Y.: The motion of a close earth satellite. Astron. J. **64**, 367–377 (1959)

Lara, M., San-Juan, J.F., López-Ochoa, L.M.: Delaunay variables approach to the elimination of the perigee in artificial satellite theory. Celest. Mech. Dyn. Astron. **120**(1), 39–56 (2014)

Lyddane, R.H.: Small eccentricities or inclinations in the Brouwer theory of the artificial satellite. Astron. J. **68**, 555–558 (1963)

Mittleman, D., Jezewski, D.: An analytic solution to the classical two-body problem with drag. Celest. Mech. **28**, 401–413 (1982)

Parks, A.D.: A Drag-Augmented Brouwer–Lyddane Artificial Satellite Theory and Its Application to Long-Term Station Alert Predictions. Technical Report NSWC TR 83–107, Naval Surface Weapons Center, Dahlgren, VA, Apr 1983

Roy, A.E.: Orbital Motion. CRC Press, New York (2004)

Schaub, H., Junkins, J.L.: AIAA education series. In: Analytical Mechanics of Space Systems. American Institute of Aeronautics and Astronautics, New York (2003)

Vallado, D.A., McClain, W.D.: Fundamentals of Astrodynamics and Applications. Microcosm Press, Space technology library (2001)

Vinh, N.X., Longuski, J.M., Busemann, A., Culp, R.D.: Analytic theory of orbit contraction due to atmospheric drag. Acta Astron. **6**, 697–723 (1979)

Vinti, J.P.: Theory of the orbit of an artificial satellite with use of spheroidal coordinates. Astron. J. **65**, 353–354 (1960)